Journal of Applied Mechanics and Technical Physics, Vol. 36, No. 1, 1995

ANALYSIS OF FLOW CHANGES IN A DIFFUSER BOUNDARY LAYER IN TERMS OF THE MAXIMUM STABILITY OF AVERAGED TURBULENT FLOWS

S. S. Dmitriev

UDC 532.526.001.5

Changes in velocity profiles were investigated experimentally in a turbulent boundary layer at a diverging wall in a flat asymmetrical diffuser duct.

For attached flow in the duct, it is shown that the velocity distribution follows the same universal logarithmic function as for a flow with a zero pressure gradient; as the divergence angle of the duct is increased, the value of the constant in this function decreases downstream.

It is also shown that flow separation is a transition to a new stable state, when the classic flow at the wall boundary layer cannot adequately counteract the positive pressure gradient which is determined by the duct geometry.

1. Depending on the nature of the reaction to the positive pressure gradient, the turbulent boundary layer can separate into two flow regions: an inner wall region ($Y = y/\delta < 0.2$) and an external region ($Y > 0.2$). Here y is the distance from the wall, and δ is the physical thickness of the boundary layer. Three main flow zones are distinguished near the wall [1]: a viscous sublayer next to the wall; a transition zone, where viscous friction forces are on the same order as the turbulent stresses of Reynolds friction; and an inner turbulent region, which occupies 10 to 20% of the thickness of the boundary layer according to various estimates, where the velocity distribution follows a universal logarithmic law

$$\frac{U}{u_\tau} = 5{,}75 \lg\left(\frac{yu_\tau}{\nu}\right) + C. \tag{1.1}$$

Here U is the longitudinal component of the average velocity at a distance y from the wall; $u_\tau = (\tau_\omega/\rho)^{1/2}$ is the dynamic velocity; τ_ω is the tangential stress at the wall; ρ is the density; ν is the kinematic viscosity; and the constant C depends on the surface state ($C = 5.5$ for hydraulically smooth surfaces).

The time for the outer part of the layer to react to a local pressure gradient dP/dx is finite and corresponds to the displacement of the flow by tens of boundary-layer thicknesses. Therefore the velocity distribution in this region depends both on local conditions and on previous flow developments, so there is no fixed relationship between the shape of the velocity profile and the local value of dP/dx. The so-called equilibrium boundary layers are an exception; their existence under positive pressure gradients was first observed by Clauser [2].

For a given pressure distribution, the velocity distribution for equilibrium layers corresponds to the function

$$\frac{U_\infty - U}{u_\tau} = f\left(\frac{yu_\tau}{\delta_1 U_\infty}\right), \tag{1.2}$$

where U_∞ is the velocity at the outer edge of the boundary layer and δ_1 is the thickness of the displacement.

The part of the layer next to the wall reacts very quickly to flow perturbations on the wall side [3], but returns to the conditions of unperturbed flow just a short distance into the flow from the origin of the perturbation. At the same time, external perturbations, including a positive pressure gradient, have no effect on the wall flow within limits. The proof of this is that the velocity distribution at the wall maintains universal conditions of similitude for large positive pressure gradients [4].

Moscow. Translated from Prikladnaya Mekhanika i Technicheskaya Fizika, No. 1, pp. 52-64, January-February, 1995. Original article submitted September 2, 1993, revision submitted March 25, 1994.

0021-8944/95/3601-0050$12.50

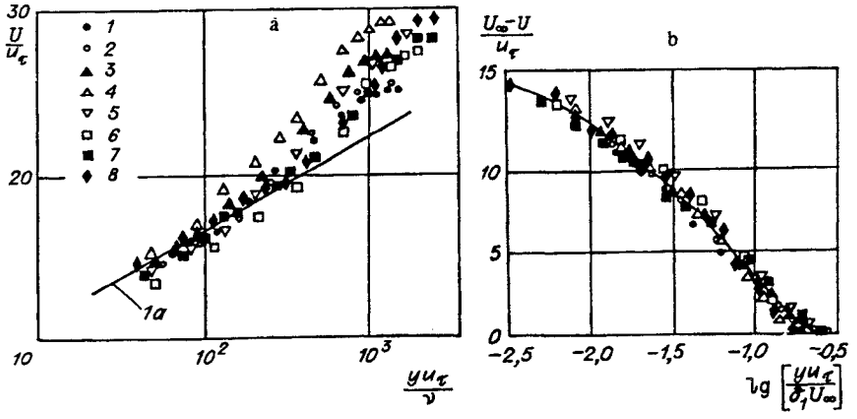

Fig. 1

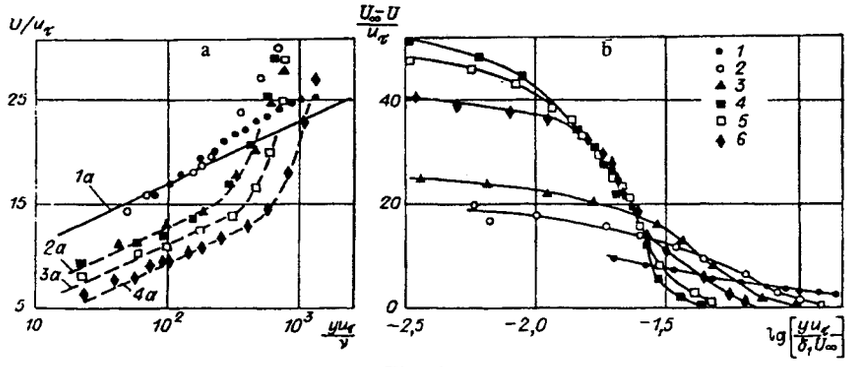

Fig. 2

These properties agree with S. S. Kutateladze's concept of the conservation of wall turbulence [5]. The related maximum-stability principle [6] allows us to distinguish theoretically a class of velocity profiles in the flow near the wall, which are most likely to be realized for a given perturbation. In other words, the average turbulent flow can be formally subjected to perturbations of one kind or another, just as in the stability of laminar flow. While the maximum-stability principle undoubtedly will be widely applied in its general formulation [7] in the future, currently it has only been used in the simplest quasi-laminar approximation [8]. Nonetheless, the very idea of maximum stability has already been used successfully to explain the behavior of flow in a turbulent boundary layer.

In this regard there is undoubted interest in both an experimental investigation and the corresponding analysis of how a positive pressure gradient changes velocity profiles and other characteristics in the boundary layer.

The boundary layer has different properties near the wall and in its outer parts, so changes which arise from a positive pressure gradient must be examined separately. Here, for all cases investigated the velocity distribution is plotted both in the coordinates $U/u_\tau = f(y \cdot u_\tau/\nu)$ for flow near the wall and in the coordinates $(U_\infty - U)/u_\tau = f(y \cdot u_\tau/\delta_1 U_\infty)$ for the whole layer.

However, flows with $dP/dx > 0$ have an intermediate region for which the average velocity follows a "square root law" [9]. Therefore, before the flow separates, the velocity distribution in the boundary layer is also plotted in coordinates $U/U_\infty = f\{(y/\delta_P)^{1/2}\}$, where $\delta_P = \tau_\omega \cdot |\, dP/dx \,|^{-1}$.

2. The research was done in a flat asymmetric diffuser duct, which had been used previously [10-12].

A 500 mm long upstream duct which contained a converging section which transitioned smoothly into a duct of constant cross section was attached to the diffuser section in order to develop a turbulent boundary layer ahead of the diffuser section. The diffuser section was made asymmetric in order to localize the flow separation (when it arose) to the diverging wall, which was made from a 57 × 270 mm flat plastic plate which had a hinged connection with the wall of the upstream duct.

The diffuser section had the following geometric relationships: $a/h_1 = 1.0$ and $0.38 \leq a/h_2 \leq 1.0$ so that the divergence angle α could be varied. Here $a = 57$ mm is the distance between the side (parallel) walls, and h_1 and h_2 are the heights of the inlet and outlet cross sections of the diffuser.

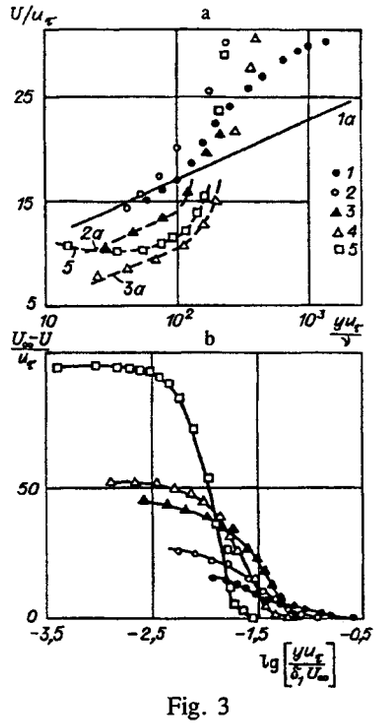

Fig. 3

A differential water manometer with an accuracy of 2 mm of water was used to measure the pressure distribution along the centerline of the diverging wall through a set of 0.5 mm diameter holes 5 mm apart. Then the experimental function P = P(x) was approximated by the least-squares method using a spline which had continuous first and second derivatives. The root mean square error of the approximation was less than the measurement error in all cases investigated. The value of dP/dx = f(x) was obtained from the resultant P(x).

The longitudinal component of the average velocity in the boundary layer was measured along the centerline of the diverging wall by using a flattened Pitot tube with outer dimensions of 0.3 × 1.0 mm. The tube was introduced into the boundary layer from the opposite wall using a micrometer, which allowed the distance from the wall to be measured with an accuracy up to 0.05 mm. A special locating device moved the tube along the wall and rotated it in two planes (parallel and perpendicular to the diverging wall).

The pressure difference between the Pitot tube and the static-pressure samplings was determined by a differential water manometer with an accuracy of 2 mm water. An alcohol micromanometer with an accuracy of 0.1 mm water was used near the wall where the velocities were small.

The value of δ was determined as the distance from the wall at which $U = 0.99 \cdot U_\infty$. The thickness of the displacement δ_1 and the momentum-loss thickness δ_2 were calculated using standard integral functions [1] from the experimental function U = U(y). The resultant relative error in δ_1 and δ_2 was no more than 3%.

The velocity field and the flow direction were measured in four evenly spaced cross sections of the diffuser section, including the inlet and outlet cross sections. The measurements were done using a triple-pointed cylindrical nozzle 2 mm in diameter, which was made in accordance with Gorlin's recommendations [13]. A special locating device, which was clamped to a lateral wall of the duct, allowed the nozzle to be placed at any point within the cross section to an accuracy of 0.5 mm. The same nozzle was used to measure the flow direction in the boundary layer along the centerline of the wall and in planes parallel to it. This was done by inserting the nozzle into the boundary layer using the locating device used for the Pitot tube.

Measurements made in this manner established that the velocity field in the flow core at the diffuser inlet was uniform and symmetric relative to the duct plane of symmetry, which passed through the centerline of the diverging wall.

Attached flow conditions were realized in the diffuser for the range $1.0 \leq n = h_2/h_1 \leq 2.0$. As $n > 2.0$, flow separation was recorded at the diverging wall, first near the outlet, and then closer to the inlet section as n increased.

The pressure ratio $\varepsilon_2 = P_2/P_0$ (where P_2 is the pressure at the diffuser outlet and P_0 is the total stagnation pressure at the duct inlet) was held constant on the order of 0.971 in all the experiments for various values of n.

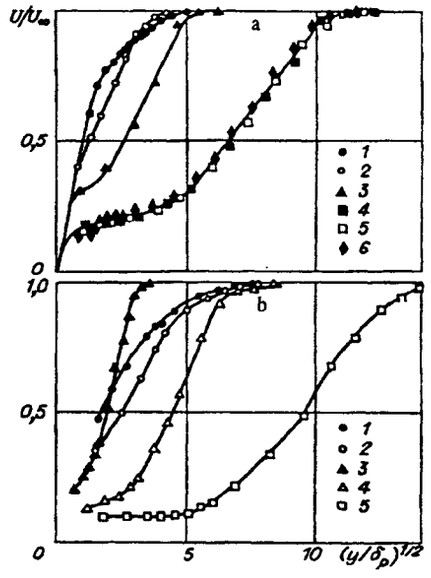

Fig. 4

The working fluid was air from a centrifugal compressor. The air entered the duct through a 500 mm diameter equilibration tank which contained two series of screens to even the flow at the inlet to the experimental duct. The air flow rate was measured by a standard nozzle, which was made in accordance with recommendations by Preobrazhenskiĭ [14].

The measurements were done for expansion ratios n = 1.3, 2.0, 2.4, and 2.65, which corresponded to divergence angles α = 3.6, 12.2, 17.2, and 20.4°. The dimensionless velocity λ in the flow core at the diffuser inlet varied within the range of 0.26-0.31; thus the effect of compressibility could be neglected.

The Reynolds number Re, calculated along the length of the upstream section and the core flow velocity at the inlet cross section of the diffuser section was $2.8 \cdot 10^6$, $3.3 \cdot 10^6$, $3.1 \cdot 10^6$, and $2.6 \cdot 10^6$, respectively for these expansion ratios.

The value of τ_ω was calculated from the Ludwieg–Tillman formula [4]

$$\tau_\omega = 0{,}123 \cdot 10^{-0{,}678H} \left(\frac{U_\infty \delta_2}{\nu}\right)^{-0{,}268} \rho U_\infty^2. \tag{2.1}$$

Here $H = \delta_1/\delta_2$ is the boundary layer form factor. The form of Eq. (2.1) does not satisfy the condition $\tau_\omega = 0$ at the separation point, but it describes boundary-layer test data for attached flow well enough [15], while values of τ_ω calculated from (2.1) for $H > 2.5$ are very small. However, an error analysis of Eq. (2.1) shows that the relative error in τ_ω grows sharply as H increases. For expansion ratios of n = 1.3 and 2.0, the relative error in τ_ω did not exceed 4.5% and 7%, respectively, for all cases investigated.

For n = 2.4 and 2.65, the relative error in τ_ω, obtained from Eq. (2.1), did not exceed 8% in regions of stable attached average flow in the boundary layer, as shown by Dmitriev [11] for these cases using the Sandborn–Klein method [15]. However, as the flow becomes unstable and separated, the error starts to grow rapidly as H increases; therefore the calculated values of τ_ω in this case give only a qualitative conclusion on the type of flow.

3. Figure 1 shows the velocity distribution in the boundary layer at the diverging wall for n = 1.3. The experimental points 1-8 correspond to cross sections X = x/L = 0.02, 0.06, 0.18, 0.29, 0.41, 0.55, 0.83, and 0.97, where x is the coordinate along the diverging wall and L is its length.

According to Gol'dshtik and Shtern [8], Eq. (1.1) determines the most stable velocity distribution for zero-gradient flow in the wall region outside the viscous sublayer and the transition region. In Fig. 1a, this function is shown by the line 1a (C = 5.5). With only a small scatter, the experimental points are located on the line 1a for $Y \leq 0.1$ at cross sections X = 0.02, 0.06, and 0.18. For X = 0.29, Eq. (1.1) is satisfied only for a distance $Y \cong 0.06$ from the wall, and the experimental points that correspond to the outer section of the boundary layer fall much farther from the line 1a than they do in the other cross sections.

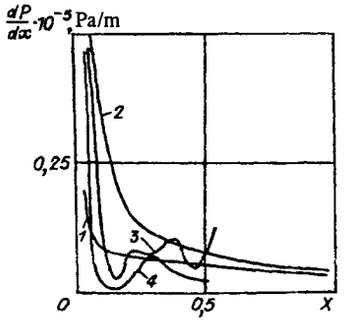

Fig. 5

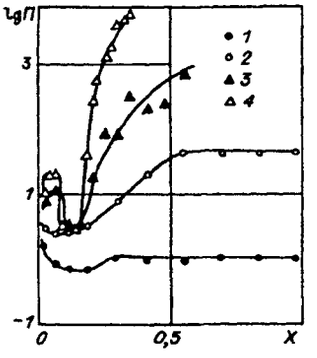

Fig. 6

In this case the largest value of dP/dx occurs for X = 0.02, after which it decreases monotonically as X increases [the corresponding function dP/dx = f(x) is shown as curve *1* in Fig. 5]. Here the velocity distribution in the cross section at X = 0.29 illustrates the inertia discussed above. When that occurs the outer part of the layer reacts on the local pressure gradient.

At X = 0.41 the universal logarithmic velocity-distribution function (1.1) again is followed to a distance Y ≅ 0.1 from the wall. However, it should be noted that the experimental points drop below the line 1a for X = 0.41 and even more so for X = 0.55, which indicates a lower value of C in (1.1).

It is not impossible that the deviation of these experimental points from the initial line 1a comes from errors in conducting and analyzing the experiment, especially because the deviation is small.

At X = 0.83 and 0.97 the experimental points again correspond with the line 1a: for Y ≤ 0.13 at X = 0.83 and for Y ≤ 0.16 at X = 0.97.

Thus, this example indicates that the velocity distribution for stable attached flow in the completely turbulent wall region of the boundary layer is determined by Eq. (1.1) with C = 5.5 as the flow develops downstream and that maximum stability occurs near the wall region in this case.

For n = 1.3, the experimental points for all cross sections lie with some scatter on one curve $(U_\infty - U)/u_\tau = f(y \cdot u_\tau/\delta_1 U_\infty)$ (Fig. 1b). This indicates that the flow is almost at equilibrium for this pressure gradient; i.e., it is energetically balanced in all cross sections.

Figure 2 shows the velocity distribution in the boundary layer for n = 2.0. The experimental points 1-6 correspond to cross sections with X = 0.02, 0.18, 0.29, 0.69, 0.83, and 0.97. The line 1a in Fig. 2a corresponds to Eq. (1.1) with C = 5.5.

For X = 0.02 and 0.18, the velocity distribution follows Eq. (1.1) for Y ≤ 0.1, and the experimental points coincide with the line 1a.

Downstream, from X = 0.29 to X = 0.69, Eq. (1.1) is followed for Y ≤ 0.08 and 0.06 respectively. However, the value of C is smaller (line 2a in Fig. 2a). For X = 0.83 and 0.97, the velocity distribution deviates even more from the initial one. The general Eq. (1.1) is followed in these cross sections for Y ≤ 0.1 and 0.12, respectively; however the constant C decreases even more (lines 3a and 4a in Fig. 2a). For X = 0.97, C is on the order of 2.3.

An analogous decrease in the viscous sublayer for diffuser flow has been obtained earlier [16]. It has also been shown [17] that the thickness of the viscous sublayer of the boundary layer decreases downstream.

The measurements described above did not allow us to obtain direct data on the velocity distribution in the region of the viscous sublayer. However, it can be assumed from earlier results [16, 17] that the deviation from the velocity distribution, determined by Eq. (1.1) with C = 5.5, indicates a decrease in the thickness of the viscous sublayer.

From Fig. 2b it can be seen that the velocity distributions deviate significantly from the initial one over the whole layer thicknesses as the flow develops downstream. However, it should be noted that for X = 0.69, 0.83; and 0.97, where $-1.9 \le \lg(y \cdot u_\tau/\delta_1 U_\infty) \le -1.6$, the experimental points lie close to a single curve in the range 0.15 ≤ Y ≤ 0.55.

This fact and the occurrence of equilibrium flow for n = 1.3 evidently result from features of the pulsating motion in the boundary layer for diffuser flow.

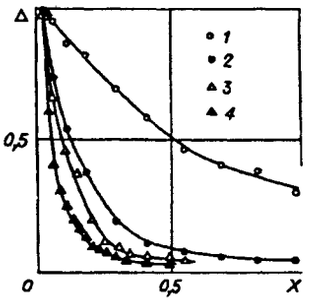

Fig. 7

Today a large volume of experimental data has been accumulated [18-24] which uniquely shows that turbulent energy is produced in two independent regions in the cross section of the turbulent boundary layer.

The first region is located directly next to the wall, as it is for the turbulent layer with zero pressure gradient, while the second is in the outer part of the layer. Depending on the data, this region lies in the range $0.25 \leq Y \leq 0.35$ [20], $0.4 \leq Y \leq 0.6$ [21, 22], or $Y \cong 0.5$ [24].

The pulsation intensity and the generation of turbulent energy both increase with distance from the diffuser inlet. Evidently this zone of turbulent energy generation is what equilibrates the boundary layer flow for $n = 1.3$ and causes local equilibrium in the outer part of the layer for $n = 2.0$.

Figure 3 shows the velocity distribution in the boundary layer at the diverging wall with $n = 2.4$. The experimental points 1-5 correspond to cross sections $X = 0.02$, 0.06, 0.154, 0.2 and 0.294.

Complete or stable separation of the boundary layer from the wall does not occur immediately [15]. It is preceded by a state of alternating or unstable separation, in which a zone with reverse flow arises and vanishes near the wall. The fraction of time in which flow is reversed (the alternation factor) increases downstream.

In this case the boundary layer is in a region of stable attached flow for $X < 0.22$, while a transition to unstable separation occurs for $X > 0.22$ [11].

The experimental points for $X = 0.02$ and 0.06 and $Y \leq 0.05$ fall on the line 1a, which is calculated from Eq. (1.1) with $C = 5.5$. For $X = 0.154$ and 0.2 and $Y \leq 0.06$ and 0.05, respectively, the velocity distribution follows Eq. (1.1), but the value of C is reduced (lines 2a and 3a in Fig. 3a).

The breakdown of Eq. (1.1) is first observed for $X = 0.294$ (curve 5), and the universal logarithmic velocity distribution in the wall region of the layer breaks down even more for $X > 0.294$, as shown by calculations of τ_ω from Eq. (2.1), and also of U/u_τ and $y \cdot u_\tau/\nu$.

When the velocity distribution is plotted as the function $(U_\infty - U)/u_\tau = f(y \cdot u_\tau/\delta_1 U_\infty)$ for $n = 2.4$, it deviates from the initial function more and more as X increases, and non-equilibrium flow occurs in the outer part of the layer.

These examples (Figs. 1-3) show that the velocity distribution in the completely turbulent wall-region of the layer is determined by Eq. (1.1) for attached average-flow conditions in the boundary layer for diffuser flow, and that when Eq. (1.1) is followed it can be taken as evidence of universal energy equilibrium. As the pressure gradient defined by the duct geometry increases (as the divergence angle α increases) and as the distance from the duct inlet increases, the constant C in (1.1) will decrease monotonically if Eq. (1.1) is followed, as noted in [16].

The velocity distribution also follows Eq. (1.1) for separated conditions ($n > 2.0$) for some distance from the inlet cross section; however the value of the constant C decreases faster than for attached conditions (see Figs. 2a and 3a for identical values of X). The universal logarithmic function (1.1) breaks down in the wall region at some stage in the flow development, which indicates that energy equilibrium breaks down in this region. However, this breakdown occurs long before the separation itself. In particular, it has been shown [11] that complete flow separation occurs in the cross section $X = 0.62$ for $n = 2.4$.

Figure 4 shows the distribution of average velocities in the boundary layer in the coordinates $U/U_\infty = f\{(y/\delta_p)^{1/2}\}$. The experimental points 1-6 in Fig. 4a correspond to the cross sections $X = 0.02$, 0.18, 0.29, 0.69, 0.83, and 0.97 for $n = 2.0$, while the points 1-5 in Fig. 4b correspond to $X = 0.02$, 0.06, 0.154, 0.2, and 0.294 for $n = 2.4$.

It is interesting to note that for $n = 2.0$, the experimental points for $X = 0.69$, 0.83, and 0.97 lie on a single curve with little scatter over the whole layer thickness, but the relative velocity depends linearly on $(\bar{y}_p)^{1/2} = (y/\delta_p)^{1/2}$ in the region $5 \leq (\bar{y}_p)^{1/2} \leq 10$, which corresponds to $0.15 \leq Y \leq 0.55$. This means that δ_p and $u_p = [(dP/dx) \cdot y/\rho]^{1/2}$ are characteristic

scales which determine the nature of the flow in this region in the boundary layer. Here u_p is the dynamic velocity of the pressure gradient. The nature of the velocity distribution in Fig. 4a confirms that the flow is in equilibrium in the outer part of the boundary layer for n = 2.0 in the cross sections X = 0.69, 0.83, and 0.97; it also confirms the results of earlier analyses [9, 25] of boundary-layer flow with a positive pressure gradient.

As can be seen from Fig. 5 (curve 3), when n = 2.4 the change of dP/dx is wave-like in the transition region to unstable separation. In this case the "square root law" [9] is not satisfied in the turbulent boundary layer, which confirms the velocity distribution for n = 2.4 shown in Fig. 4b.

4. Figure 5 shows the distribution of dP/dx along the diverging wall. Curves 1-4 correspond to expansion ratios of n = 1.3, 2.0, 2.4, and 2.65.

Gogish and Stepanov [26] present all the most widely used local separation criteria in the form

$$\frac{z}{\rho U_\infty^2}\frac{dP}{dx} \geqslant B\mathrm{Re}^{-1/m}, \tag{4.1}$$

where z is the characteristic thickness of the boundary layer, and B and m are constants determined empirically as a function of the Mach number and Re. If $z = \delta_1$ and Re is large enough, which is true in this case, then B = 0.015 and $m = \infty$ [27]. Under these assumptions, the inequality (4.1) takes the form

$$\frac{\delta_1}{\rho U_\infty^2}\frac{dP}{dx} \geqslant 0{,}015. \tag{4.2}$$

By multiplying the left and right sides of (4.2) by $\rho \cdot U_\infty^2/\tau_\omega$, we obtain

$$\Pi = \frac{\delta_1 dP/dx}{\tau_\omega} \geqslant \frac{0{,}03}{c_f}. \tag{4.3}$$

The inequality (4.3) defines the conditions for separation to occur. Generally speaking, the parameter Π is used as the characteristic for the flow gradient. However, it has been shown [23] that Π can be used as a measure of flow stability in the boundary layer. In this sense the inequality (4.3) can serve as a stability criterion for the existence of separated and attached flows in the boundary layer.

Two stable flow states are possible in diffuser ducts: attached flow and separated flow. Here "stability" should be understood to mean that separated flow always occurs under certain conditions.

The stability of these two flow types is confirmed by the presence of hysteresis effects when external phenomena change the flow from attached to separated and back again. One example [28] is the case of flow in a circular duct with injection normal to the external walls. When the external diffuser walls diverged at an angle of $\alpha = 50°$ and the injected flow was on the order of 5%, energy losses were reduced by 35%, and attached flow was established at the diffuser walls.

However, when the relative injected fluid was reduced to 2-2.5%, the losses increased abruptly and the flow switched to separated. This unique hysteresis points to the significant stability of both separated and attached flow.

In this case, the value of Π at the diffuser inlet cross section (X = 0.02) changed almost instantaneously from 0 to 1.55, 3.1, 7.84, and 10.7 for n = 1.3, 2.0, 2.4, and 2.65, respectively.

Figure 6 shows the change in Π along the diverging wall. Curves 1-4 correspond to the expansion ratios n = 1.3, 2.0, 2.4, and 2.65.

The condition $\Pi < 0.03/c_f$ is fulfilled at X = 0.02 and all n; i.e., the initial attached flow in the boundary layer can be considered stable, according to accepted concepts. Then Π should decrease downstream in all cases, according to the maximum-stability principle [7]. Indeed, Π did decrease for all n in the initial section of the duct; for n = 2.4 and 2.65 the decrease was rather large for $0.1 < X < 0.2$ (to Π on the order of 3.5).

An analysis of the structure of the parameter Π shows that this can occur when δ_1 decreases, τ_∞ increases, or dP/dx decreases. The first two conditions are impossible in diffuser ducts with no external perturbations. Consequently in this case a decrease in Π comes directly from a decrease in dP/dx. However, it is known that growth of the boundary layer substantially

changes dP/dx over what can be determined considering only the duct geometry, especially ahead of the separation. Then the changes in δ_1 and $d\delta_1/dx$ must be analyzed in order to determine how they affect the flow separation mechanism.

5. In order to make the discussion clear and simple, it is convenient to analyze the one-dimensional flow of an incompressible fluid. For a qualitative analysis we can assume without loss of accuracy that there are no boundary layers on the lateral (parallel) walls or on the straight wall opposite the one which diverges. Then the equations of motion and continuity are written in the form

$$\frac{dP}{dx} = -\rho c \frac{dc}{dx}; \tag{5.1}$$

$$G = \rho a h_e c. \tag{5.2}$$

From (5.1) and (5.2), dP/dx can be represented as

$$\frac{dP}{dx} = \frac{G^2}{\rho a^2 h_e^3} \frac{dh_e}{dx}, \tag{5.3}$$

where c is the velocity in the flow core in a cross section at x along the diverging wall; G is the mass flow rate through the duct, and h_e is the effective height of the cross section. According to these assumptions, the effective height of the cross section at x is $h_e = h_1 + x \cdot \sin\alpha - \delta_1/\cos\alpha$.

Then (5.3) takes the form

$$\frac{dP}{dx} = \frac{G^2[\sin\alpha - (d\delta_1/dx)(1/\cos\alpha)]}{\rho a^2 (h_1 + x\sin\alpha - \delta_1/\cos\alpha)^3}. \tag{5.4}$$

From (5.4) it can be seen that the growth of boundary layers affects dP/dx nonuniformly. With a constant flow rate through the duct, the value of dP/dx in the same cross section of the boundary layer (x = const) increases when δ_1 increases but decreases when $d\delta_1/dx$ increases.

Figure 7 shows the change in the quantity $\Delta = \delta_{10}/\delta_{1x}$ along the diverging wall. Curves 1-4 correspond to expansion ratios n = 1.3, 2.0, 2.4, and 2.65. Here δ_{10} is the thickness of the displacement at X = 0.02 and δ_{1x} is the thickness of the displacement in the cross section at X.

As can be seen from Fig. 7, $d\delta_1/dx$ is much larger for separated conditions (n > 2.0) than for attached conditions. Namely this can explain the very sharp decreases in dP/dx for n = 2.4 and 2.65 in the initial section of the duct (see Fig. 5), where δ_1 is relatively small. In turn, the sharp decrease in dP/dx causes a decrease in Π in this region, as shown by the tendency of the flow in the boundary layer to maintain its initial state; i.e., by the realization of the maximum-stability principle in this case.

Of course, if $d\delta_1/dx$ is large downstream, δ_1 starts to increase rapidly, and therefore dP/dx should increase according to (5.4).

Here we should examine one feature of the change in dP/dx along the diverging wall for separated flow conditions (n = 2.4 and 2.65). As can be seen from Fig. 5, after a sharp decrease in dP/dx, a local increase in dP/dx is observed in both cases in the initial section of the duct at X > 0.15. According to local separation theory [26], the local increase in dP/dx is induced by the interaction of the boundary layer with the external flow. However, boundary-layer separation of an incompressible fluid is a rather complicated transition process from stable attached flow to a completely developed separation, and is not localized in a region of a local pressure increase [29]. The shape of the distribution of dP/dx in Fig. 5 is experimental confirmation of this theoretical conclusion [29]. Measurements in the boundary layer [11] have shown that complete separation of the boundary layer starts at cross sections X = 0.62 and 0.41 for n = 2.4 and 2.65, respectively.

As δ_1 grows, the outer region where turbulence energy is generated, which coincides with the zone in which turbulent stresses pass through a maximum, falls at a larger and larger distance from the wall, and less and less energy reaches the wall. At the same time the wall region needs more energy input to move fluid against the increasing pressure. As shown above, this input comes from the strengthening of the pulsating motion and the growth of energy production in the outer part of the layer.

When transverse transport equilibrates the energy-production and dissipation processes in the wall zone, the initial attached average flow in the boundary layer remains in equilibrium downstream. Here this occurs for n = 1.3 and 2.0, the condition $\Pi < 0.03/c_f$ is fulfilled along the length of the diverging wall, and a constant value of Π is established when $X > 0.3$ and 0.55 for n = 1.3 and 2.0, respectively.

If these processes do not equilibrate, then Π grows without bound downstream [23]. The value of Π is on the order of 10^3 and $6 \cdot 10^3$ in the cross sections X = 0.55 and 0.35 for n = 2.4 and 2.65. The inequality (4.3) is satisfied when $X > 0.41$ for n = 2.4 and when $X > 0.27$ for n = 2.65, and the attached flow becomes unstable.

6. The profile of the averaged velocity in the turbulent boundary layer always undergoes a characteristic deformation in the zone $0.2 < Y < 0.4$ ahead of the separation regions for diffuser flow.

Analysis of the equations of motion [30] shows that this deformation is directly related to the tendency of the flow to remain attached, because it tends to increase those terms of the equation of motion which equilibrate the stagnation force of the pressure. The tangential turbulent stresses, which arise in the wall region of the boundary layer in diffusion flow where $\partial\tau/\partial y > 0$, have a stabilizing role [30], which, according to the same equation of motion, also means that these stresses act against the stagnating forces of the pressure.

As the results presented here show, the processes which intensify the growth of the boundary layer, i.e., the growth of $d\delta_1/dx$ initially decrease dP/dx and consequently tend to keep the flow attached.

Generally speaking, all changes in the transition of the turbulent boundary layer to diffuser flow, including the change of the observed nature of the pulsating motion [18-24], tend to maintain the initial attached flow, because they increase the inflow to the wall of fluid layers that have a large reserve of kinetic energy and therefore are more stable with respect to separation.

However, at some stage in the flow development, as determined by the inequality (4.3), all these changes become insufficient to maintain the initial attached flow. The classic flow in the boundary layer then can no longer react adequately to external forces, determined by the duct geometry, and the flow separates.

In this regard separation can be considered a specific flow reaction which is directed to reduce the pressure gradient and which is initially determined by the duct geometry, and the separation can be viewed as a flow transition to a new stable state, because duct geometry no longer affects the nature of the flow and the pressure change in the separated flow.

REFERENCES

1. Hermann Schlichtling, Boundary-Layer Theory (translated by J. Kestin), 7th ed., McGraw-Hill, New York (1979).
2. F. H. Clauser, "Turbulent boundary layers in an adverse pressure gradient," J. Aeronaut. Sci., **21**, No. 2, 91-108 (1954).
3. P. S. Klebanoff and Z. W. Diehl, "Some features of artificially thickened, fully developed boundary layers with zero pressure gradient," Report N 1110, NACA, Washington, DC (1952).
4. H. Ludwieg and W. Tillman, "Investigations of wall shear tension in turbulent boundary layers," Ing. Arch., **17**, 288-289 (1949).
5. S. S. Kutateladze, Wall Turbulence [in Russian], Nauka, Novosibirsk (1973).
6. M. A. Gol'dshtik, "Maximum-stability principle for averaged turbulent flows," Dokl. Akad. Nauk, **182**, No. 5, 1026-1028 (1968).
7. V. M. Lyachter, "The stochastic nature of turbulent flows and approaches to a closed description of turbulence," in: Turbulent Flows [in Russian], Nauka, Moscow (1974), pp. 136-140.
8. M. A. Gol'dshtik and V. N. Shtern, Hydraulic Stability and Turbulence [in Russian], Nauka, Novosibirsk (1977).
9. B. A. Kader and A. M. Yaglom, "Turbulence in the region where the 'square root wall law' can be applied to a decelerating boundary layer," Dokl. Akad. Nauk, **242**, No. 6, 1273-1276 (1978).
10. A. E. Zaryankin, V. G. Gribin, and S. S. Dmitriev, "Investigation of the flow structure in flat diffuser ducts and a method to improve their efficiency," Izv. Vuzov Énergetika, No. 9, 87-92 (1989).
11. S. S. Dmitriev, "The mechanical separation of a turbulent boundary layer from a smooth wall," Izv. Akad. Nauk. Mekh. Zhidk. Gaza, No. 6, 69-77 (1990).
12. A. E. Zaryankin, V. G. Gribin, and S. S. Dmitriev, "Comparative efficiency of diffuser ducts with different methods of aerodynamically affecting the flow," Izv. Vuzov Énergetika, No. 4, 67-73 (1991).

13. M. S. Gorlin, Aeromechanical Measurements [in Russian], Nauka, Moscow (1964).
14. V. P. Preobrazhenskiĭ, Measurements and Instrumentation in Heat Engineering [in English, revised from the 1978 Russian edition], Mir, Moscow (1980).
15. Sandborn and Klein, "Flow models with boundary layer separation," Transactions of the American Society of Engineers and Mechanics, Engineering Mechanics (1961), pp. 3-17.
16. G. I. Efimenko and E. M. Khabakhpasheva, "Effect of a positive pressure gradient on the structure of wall turbulence," in: Gradient and Diffuser Flows [in Russian], Nauka, Novosibirsk (1976), pp. 49-65.
17. E. U. Repik and Yu. P. Sosedko, "Investigation of discontinuous flow structure in the wall region of a turbulent boundary layer," in: Turbulent Flows [in Russian], Nauka, Moscow (1974), pp. 172-184.
18. G. B. Shubauer and P. S. Klebanoff, "Investigation of separation of the turbulent boundary layer," Technical Note N 2133, NACA, Washington, DC (1950).
19. A. I. Leont'ev, E. V. Shishov, V. M. Belov, and V. N. Afanas'ev, "Average and pulsation characteristics of a hot turbulent boundary layer and heat transfer in the diffuser region," Heat Transfer in Turbulent Wall Flows, Part I, Proceedings of the 5th All-Union Conference on Heat and Mass Transfer [in Russian], Minsk (1976), pp. 77-86.
20. E. M. Khabakhpasheva, G. I. Efimenko, and Yu. A. Rudi, "Development of a shear layer in attached diffuser flow," Turbulent Jet Flows, Author Abstracts of the 4th All-Union Conference on the Theoretical and Applied Aspects of Turbulent Flows, Part 2 [in Russian], Tallin (1982), pp. 152-163.
21. A. I. Leont'ev and E. V. Shishov, "Behaviors of wall turbulence in the gradient flow region under complex thermal boundary conditions," Turbulent Wall Flows [in Russian], Novosibirsk (1984), pp. 105-111.
22. P. S. Roganov, V. P. Zabolotskiĭ, and E. V. Shishov, "Investigation of turbulent heat transfer processes in wall flows based on analysis of turbulence transport equations," Turbulent Wall Flows [in Russian], Novosibirsk (1984), pp. 121-126.
23. Julius C. Rotta, The Turbulent Boundary Layer in an Incompressible Fluid [Russian translation], Sudostroenie, Leningrad (1967).
24. P. Dengel and H. H. Fernholz, "An experimental investigation of an incompressible turbulent boundary layer in the vicinity of separation," J. Fluid Mech., **212**, 615-636 (1990).
25. S. S. Kutateladze, Analysis of Similitude in Thermophysics [in Russian], Nauka, Novosibirsk (1982).
26. L. V. Gogish and G. Yu. Stepanov, Separated Turbulent Flows [in Russian], Nauka, Moscow (1979).
27. G. M. Bam-Zelikovich, "Calculation of boundary layer separation," Izv. Akad. Nauk Otdel. Tekh. Nauk, No. 16, 68-85 (1954).
28. M. E. Deĭch and A. E. Zaryankin, Hydrogasodynamics [in Russian], Énergoatomizdat, Moscow (1984).
29. V. K. Sychev Vik, "Theory of self-induced separation of a turbulent boundary layer," Izv. Akad. Nauk Mekh. Zhidk. Gaza, No. 3, 51-60 (1987).
30. A. E. Zaryankin, V. G. Gribkin, and S. S. Dmitriev, "A mechanism of initiating flow separation from the walls of smooth ducts," Teplofiz. Vys. Temp., **27**, No. 5, 913-919 (1989).